



**HAL**  
open science

## Zero-emission casting-off and docking maneuvers for series hybrid excursion ships

Walter Lhomme, Joao Trovao

► **To cite this version:**

Walter Lhomme, Joao Trovao. Zero-emission casting-off and docking maneuvers for series hybrid excursion ships. *Energy Conversion and Management*, 2019, *Energy Conversion and Management*, 184, pp.427-435. 10.1016/j.enconman.2019.01.052 . hal-03209623

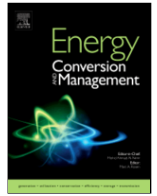
**HAL Id: hal-03209623**

**<https://hal.univ-lille.fr/hal-03209623v1>**

Submitted on 8 Jul 2024

**HAL** is a multi-disciplinary open access archive for the deposit and dissemination of scientific research documents, whether they are published or not. The documents may come from teaching and research institutions in France or abroad, or from public or private research centers.

L'archive ouverte pluridisciplinaire **HAL**, est destinée au dépôt et à la diffusion de documents scientifiques de niveau recherche, publiés ou non, émanant des établissements d'enseignement et de recherche français ou étrangers, des laboratoires publics ou privés.



## Zero-emission casting-off and docking maneuvers for series hybrid excursion ships

W. Lhomme<sup>a</sup>, J.P. Trovão<sup>b, c, \*</sup>

<sup>a</sup> Univ. Lille1, Centrale Lille, Arts et Métiers Paris Tech, HEL, EA 2697 – L2EP, Laboratoire d'Electrotechnique et d'Electronique de Puissance, F-59000 Lille, France

<sup>b</sup> Dept. of Electrical & Computer Engineering, Université de Sherbrooke, Sherbrooke, QC J1K 2R1, Canada

<sup>c</sup> INESC Coimbra, DEEC, University of Coimbra, Polo II, 3030-290 Coimbra, Portugal

### ARTICLE INFO

#### Keywords:

Electric excursion ship  
Supercapacitors  
Battery  
Zero-emission maneuvers  
Energetic Macroscopic Representation

### ABSTRACT

Ecological areas visits require appropriate management of key ecological features. In protected reserves innovative systems should be developed to facing problems of pollution, exhaust fumes and noise. These underlying conditions lead to special challenges for excursions ships. The switching to a cleaner, safer and quieter transport system seems to be a sustainable long-term solution for the problems of ecological areas, where more electric ship can be an important part of the solution and principally for the last mile. This paper presents a design approach of a hybrid Energy Storage Systems (ESS) for new generation of series hybrid excursion ship devoted to ecological areas to avoid any emission during the casting-off and the docking maneuvers. The main purpose of the paper is to show that, even if the hybrid ESS plus series-hybrid propulsion were already used to other vehicles, the gain for a ship with no regenerative capability is not evident. The proposed hybridization is built upon a fully-active parallel topology with battery and supercapacitors. The sizing methodology and the configuration of the ESS are detailed. For a real mission profile in Alster Lake (Hamburg, Germany) it is shown that a small battery pack of 2 kWh with a supercapacitor bank of 0.54 kWh are necessary to have zero-emission maneuvers. The graphical formalism Energetic Macroscopic Representation (EMR) is used to describe the model and to establish an energy analysis tool. An inversion-based control scheme is then deduced from the EMR and simulation results are provided to validate the proposed methodology. The usage of hybrid ESS avoids 1.39 kg of CO<sub>2</sub> during the casting-off and docking maneuvers despite increasing consumption of 0.21 (+ 8%). However, the plug-in capability can be introduced and a recharge of the battery when the ship is docked could reduce the global consumption and emissions by 20% in comparison to the original ship.

### Nomenclature

$C_{DC}$	DC bus capacitance [F]
$C_{i,j}(t)$	Current controller of the ESS $j$
$C_j$	Capacity of the ESS $j$ [Ah]
$\dot{C}_s(t)$	Speed controller
$C_v(t)$	DC bus controller
$f_s$	Coefficient of friction of the mechanical shaft [Nm.s]
$i_{ch,j}(t)$	Current chopper of the ESS $j$ [W]
$i_{DC}(t)$	DC bus current [A]
$i_j(t)$	Current of the ESS $j$ [A]
$i_t(t)$	Total current of the power supply system [A]
$i_{SM}(t)$	Synchronous machine current [A]
$J_s$	Moment of inertia of the mechanical shaft [kg.m <sup>2</sup> ]
$L_j$	Inductance value of the chopper $j$ [H]

$m_j$	Chopper modulation ratio of the ESS $j$ [0,1]
$p_{dem}(t)$	Total power demanded [W]
$P_{dem}$	Average of the total power demanded [W]
$p_{ICE}(t)$	ICE power [W]
$p_j(t)$	Power of the ESS $j$ [W]
$r_j$	Series resistance of the ESS $j$ [ $\Omega$ ]
$r_{L_j}$	Series resistance of the inductor of the chopper $j$ [ $\Omega$ ]
$T$	Profile mission period [s]
$t_c$	Casting-off time maneuver [s]
$t_D$	Docking time maneuver [s]
$T_{ICE}(t)$	ICE torque [Nm]
$T_{SM}(t)$	Synchronous machine torque [Nm]
$v_{ch,j}(t)$	Voltage chopper of the ESS $j$ [W]
$v_{DC}(t)$	DC bus voltage [V]
$v_j(t)$	Voltage of the ESS $j$ [V]
$v_j^{OCV}(t)$	Open-voltage of the ESS $j$ [V]

\* Corresponding author at: Dept. of Electrical & Computer Engineering, Université de Sherbrooke, Sherbrooke, QC J1K 2R1, Canada.  
Email address: Joao.Trovao@USherbrooke.ca (J.P. Trovão)



Fig. 1. Alster Lake (Hamburg, Germany) excursion ship example (). available at: <http://www.alstertouristik.de>

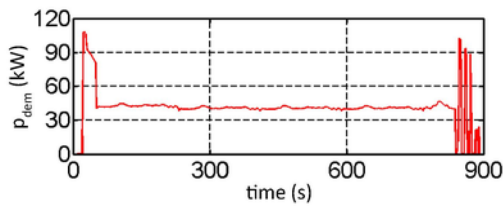


Fig. 2. Electric propulsion power demand  $p_{dem}$  of the studied excursion ship.

**Greek letters**

- $\Delta t_{on}$  On-time of the ICE operation [s]
- $\Delta t_{off}$  Off-time of the ICE operation [s]
- $\Delta W_{bat}$  Battery energy variation [Wh]
- $\eta_{ch_j}$  Chopper efficiency of the ESS  $j$  [%]
- $\eta_{SM}$  Synchronous machine efficiency [%]
- $\Omega_{SM}(t)$  Synchronous machine speed [rpm]

**Subscripts**

- $j \in \{Bat, SC\}$  Refer to an ESS: battery or supercapacitors
- $meas$  Measure value of the variable
- $ref$  Reference value of a variable

**Abbreviation**

- CO<sub>2</sub> Carbon dioxide
- EMR Energetic Macroscopic Representation
- ESS Energy Storage System
- ICE Internal Combustion Engine
- IMO International Maritime Organization
- SC SuperCapacitors

**1. Introduction**

Emissions related to maritime activities are rapidly growing due to the increasing of maritime traffic. The shipping emissions of carbon dioxide (CO<sub>2</sub>) was of 870 million of tons in 2007. In the absence of reg-

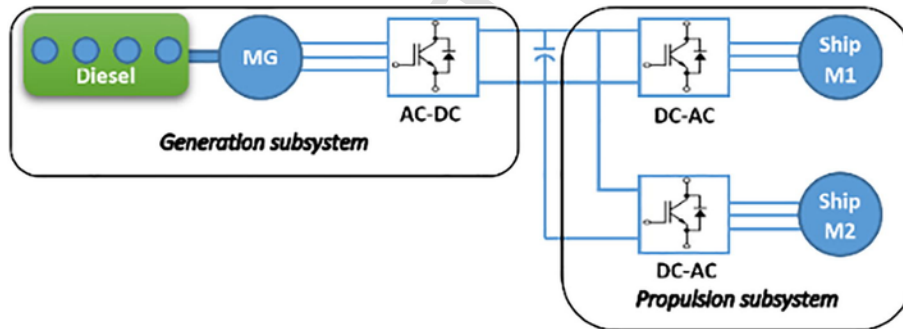


Fig. 3. Structural description of the diesel-electric ship.

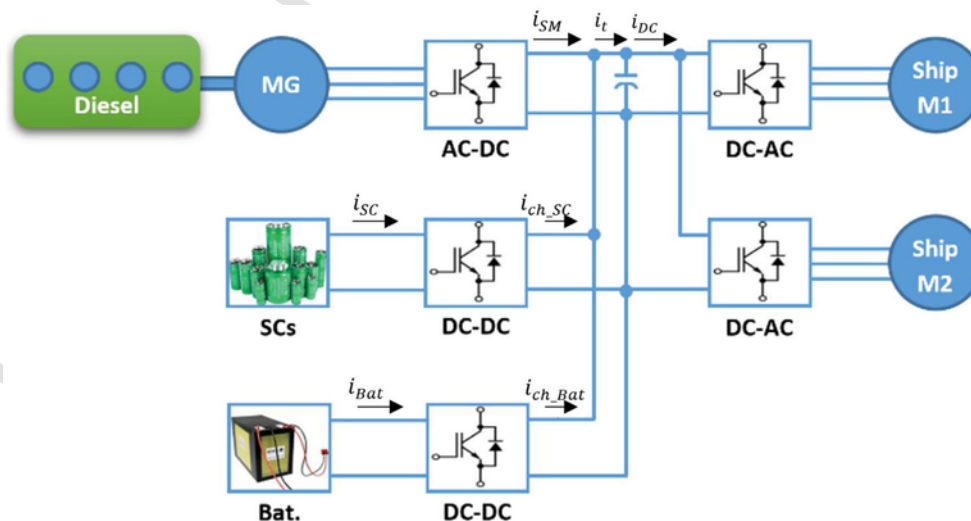


Fig. 4. Structural description of the series hybrid ship.

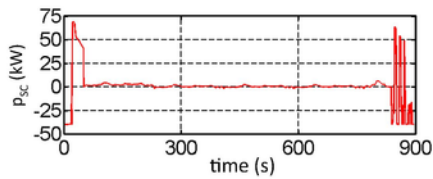


Fig. 5. Supercapacitor power profile over the considered round-trip mission.

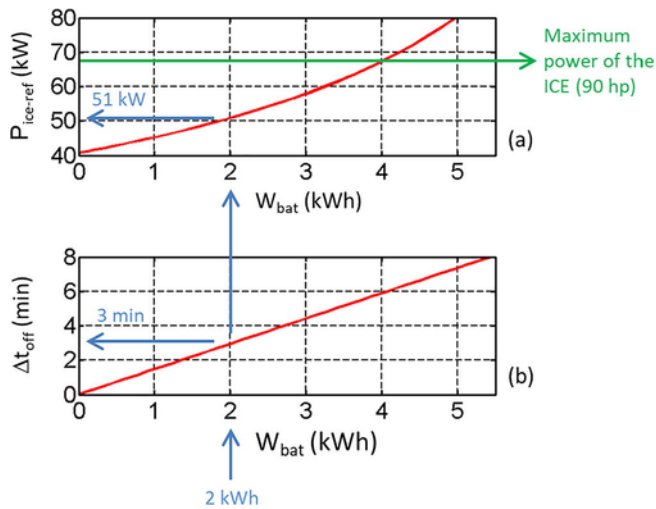


Fig. 6. Impact of the battery in the global ESS: a) variation of the ICE average power; b) off-time of the ICE operation as a function of the battery system size.

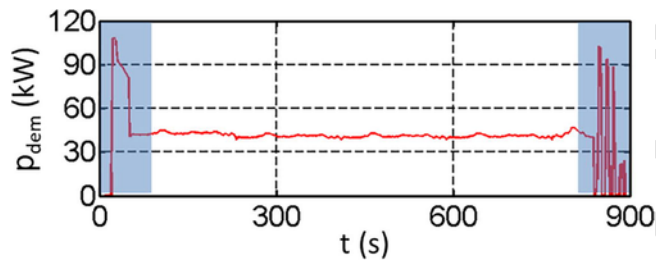


Fig. 7. Switch-off periods of the internal combustion engine considering 2kWh of battery.

ulations an increase of 200–300% of CO<sub>2</sub> is predicted by 2050. To tackle this issue, the International Maritime Organization (IMO) has defined in 2010 an “Energy Efficient plan” to reduce significantly the emissions [1,2]. New challenges must be then reached to improve ship systems in terms of energy efficiency and environmental behavior [3,4]. As stated by Hansen et al., some research and development are carried out to improve existing products and procedures or to lead to the development of new products and procedures in marine sector [5]. Electric propulsion in boats, ships and vessels is a key issue to reach a better and more sustainable transportation on the sea, rivers and lakes. Because of the massive research and development in the automotive industry, hybrid electric propulsion has now become available in maritime application. Such a system will combine the strengths of an electric drive system, an ideally designed propeller, modern energy storage systems, and the optimized use of diesel engine as a primary source of energy as discussed by Hansen et al. in [5], and also by García-Olivares et al. in [6].

The ongoing idea, like in other vehicle applications, is to maximize the global efficiency and minimize the emissions with the trend to zero emission operations in sensitive areas. Some boat prototypes have been proposed in recent literature [5–12]. A non-exhaustive survey on electric and solar boats is presented by Guellard et al. in [9]. The usability

of multiple Energy Storage System (ESS) by a passive association of battery and SuperCapacitors (SC) for an excursion ship is studied by Trovão et al. in [10], but any quantification of fuel consumption or emissions were provided. The interactions of the multiple power sources when a hybrid ESS is used are addressed by Bellache et al. in [11]. In [12], Hou et al. have studied the problem of the energy management improvement for a hybrid electric boat assisted by SC and Li-Ion battery with a fully decoupled topology. In [13], Zhou et al. have discussed and analyzed the coordination of power management strategies for a series hybrid electric boat based on dynamic load’s power distribution approach using diesel generator and battery. An electric ferry with a hybrid power system has been modeled by Monaaf et al. in [14] where the power management system was studied by simulation using the MATLAB/Simulink™ software. In [15], Lhomme and Trovão have studied the resizing of the Internal-Combustion Engine (ICE) coupled to a SC pack leads a gas consumption reduction of 9.6%, and a CO<sub>2</sub> emission reduction of 9.5%, but the zero-emission concept was not addressed. Nonetheless, the main challenge in boats is reaching consumption and emission reduction without regenerative braking, which justifies the adoption of hybrid configurations. ESS sizing and management are critical aspects to the performance and cost of and series hybrid ships. The energy management of multiple ESS is of utmost importance for promoting operational performance and enhancing system efficiency as demonstrated by Nguyen et al. in [16] for multi-source vehicle. Some preliminary insights into optimal ESS sizing and their coupling to energy management have been discussed in the literature by Shen and al. in [17], by Ostadi and Kazerani in [18], and also by Araújo et al. in [19]. Typically, power requirements are usually formulated as optimization constraints, while manufacturing cost, system efficiency, or fuel economy are often assigned as optimization objectives. Zhang et al. studied the optimal sizing of hybrid ESS as a multi-objective optimization problem considering system cost and battery lifetime in [20]. Wu et al. have proposed a convex programming framework using for optimal energy management and components sizing of a solar-battery power source for smart home in [21]. More globally, Martinez et al. in [22] have presented a comprehensive analysis of energy management strategy evolution toward blended mode and optimal control, providing a thorough survey of the latest progress in optimization-based algorithms.

Subscribed to this topic, the main objective of this paper is to propose and analyze a sizing methodology of an active association of battery and SC to avoid any local emissions for casting-off and docking maneuvers. Prior to this paper no zero-emission casting-off and docking maneuvers had ever been considered for excursion ships. The main idea is to provide a suitable solution for excursion ships that operate in very sensible areas and protected reserves, introducing the concept of emission-free last mile in excursion ships. For that, simulations using Energetic Macroscopic Representation (EMR) are addressed to evaluate the behavior of the proposed system as a results of a dedicated sizing procedure. As proposed by Bouscayrol et al. in [23], EMR is a graphical model organization tool developed to deduce systematically the control and energy management of complex energetic systems. In the past, it has been successfully used for hybrid and electric vehicles, railway traction systems and automatic subways as presented in [15,16,24,25]. Other tools, such as the well-known unified language Bond Graph, allow to describe graphically the energetic transfer for multidomain physical systems, as presented by Borutzky et al. in [26]. Nevertheless, in comparison with EMR, Bond Graph does not allow to deduce systematically the control based on the inversion of the description. It is however possible to deduce a state-space representation, which can lead to a global control.

In this scope and using as a case study an excursion ship typically used in Alster Lake, Hamburg, Germany, the zero-emission manoeuvres approach is studied to validate the proposed concept for casting-off and

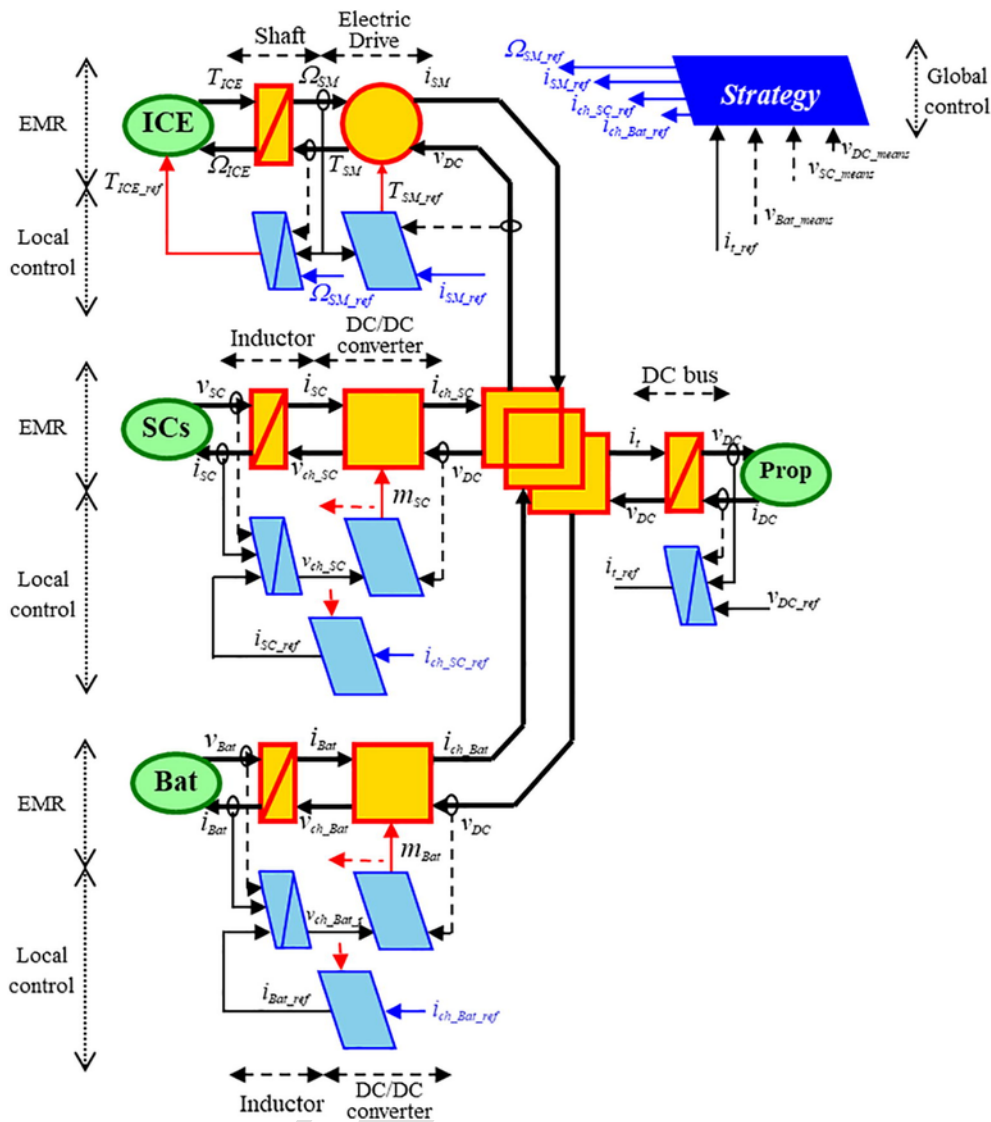


Fig. 8. Energetic Macroscopic Representation and control structure of the studied ship power system configuration.

Table 1  
System parameters.

Parameters	Variable	Values
Inductor inductances	$L_{Bat}$ $L_{SC}$	1.37 mH
Inductor parasitic resistances	$r_{LBat}$ $r_{LSC}$	28.9 mΩ
SC module's series resistance	$r_{SC}$	5 mΩ
SC module's nominal voltage	$v_{SC-nom}$	54 V
SC module's nominal capacitance	$C_{SC}$	130 F
DC bus voltage	$v_{DC}$	560 V
Battery module's series resistance	$r_{SC}$	6 mΩ
Battery module's nominal voltage	$v_{Bat-nom}$	36 V
Battery module's nominal Capacity	$C_{Bat}$	14.5 Ah

docking. Based on the initial studies presented in [10,15], the addition of a small battery pack is hereby extended using a more complete model based on EMR of the original excursion ship. The used model has been instrumental to the accurate design of the battery pack and, also, in improving the inner-control loop and the energy management strategy. A complete analysis is carried out in this paper, with an assessment of battery-SC full active hybrid topology to zero-emission maneuvers of hybrid series ship.

The remaining parts of the paper is structured as follows. The excursion ship and the proposed architecture is presented in Section 2. Section 3 addresses the ESS design for active association. The series hybrid excursion ship with multiple ESS model, control structure and energy strategy framework based on EMR approach are described in Section 4. Section 5 presents and discusses the simulation results for a real mission profile of a lake ship with specific focus on the casting-off and docking operations. The concluding remarks and ongoing works are outlined in Section 6.

## 2. Excursion ship case study

### 2.1. Original configuration

The case study considered for this zero-emission maneuver is the ship used for 15min ferry operations as presented in Fig. 1. The assumption that the casting-off and the docking operation phases should be without any emissions configures a typical issue of sensitive or protected areas. The ship has 25m of length, 5m of beam, 1.3m of draught and can carrier up to 100 passengers.

The power demanded ( $P_{dem}(t)$ ) to the supply system is presented in Fig. 2, and it is the results of on-board acquisition process during a nor-



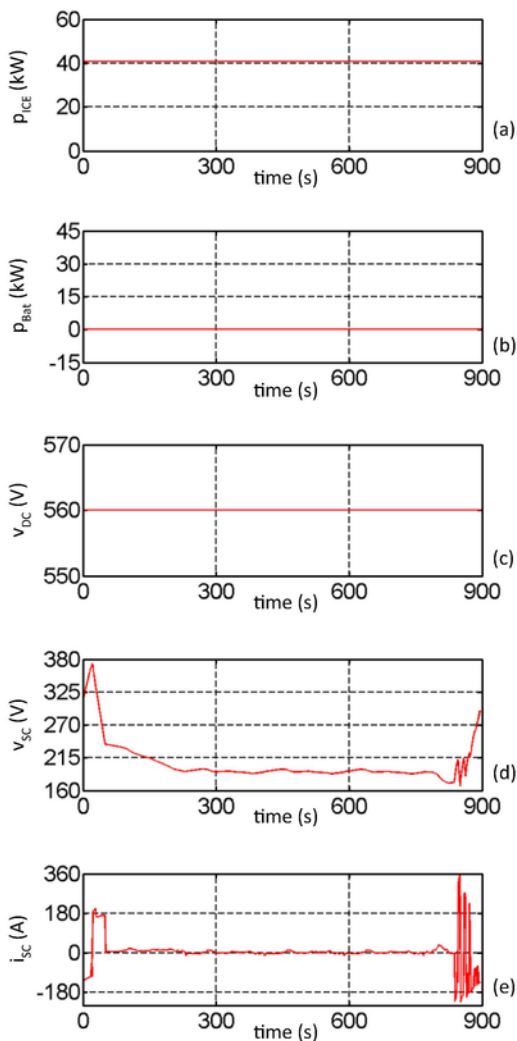


Fig. 9. Results without battery: ICE power (a), battery power (b), DC bus voltage (c), SC current (d) and SC voltage (e).

mal transport service. Unless minor variations on the power demand profile, all the tips have the same pattern. Analyzing this pattern, four main operations could be identified:

- Standby: used to pick up and drop passengers (before 20s and after 890s);
- Casting off: take the ship of its quasi-immobility to its cruising speed (20–50s);
- Cruising speed: nearly constant power demanded to transit at constant speed (50–830s);
- Docking: fastest dynamics with several variations from 0 to 100kW (830–890s).

In this paper, a diesel-electric topology is used as the original configuration. The overall description corresponds to a propulsion subsystem and a generation subsystem (diesel-electric generator 200 hp) plugged to a common DC bus, as presented in Fig. 3.

2.2. Series hybrid configuration

An active association of a pack of battery and SC has been considered to keep a full-electric operation during the casting off and the

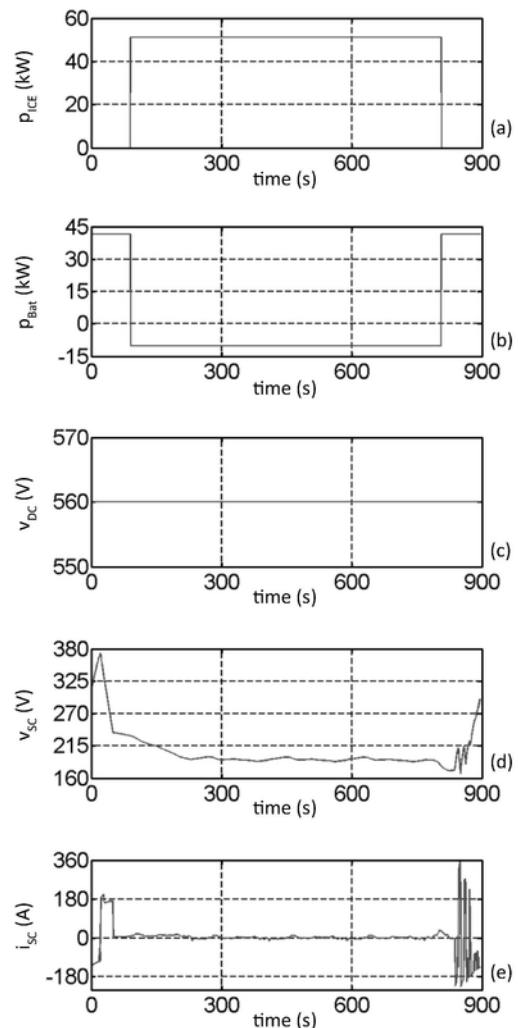


Fig. 10. Results with battery (zero-emission maneuvers): ICE power (a), battery power (b), DC bus voltage (c), SC current (d) and SC voltage (e).

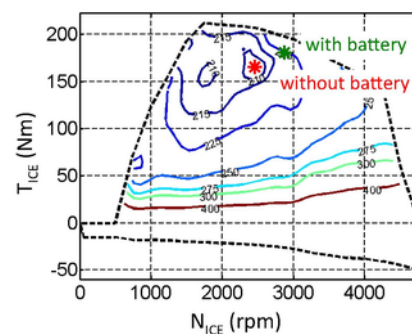


Fig. 11. Operating points of the ICE (90 hp) with and without battery for the results of Figs. 9 and 10.

docking phases. The proposed hybrid configuration is presented in Fig. 4. Considering the power demand diagram and the proposed series hybrid propulsion system with the active association of battery and SC, the ESS must be sized to provide the power demanded by all the operations of the ship.

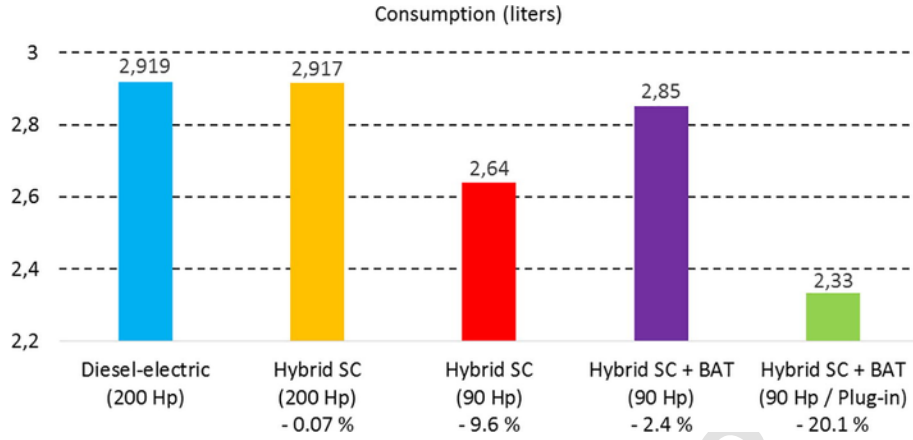


Fig. 12. Fuel consumption analysis.

### 3. Design of the energy storage system

#### 3.1. Sizing of the supercapacitors system

The power requested to the diesel-generator should be the average power of the mission cycle (Fig. 2) due to the buffer operation induced to the SC and battery. The power balance of the ship power system is proposed in (1):

$$P_{dem}(t) = P_{ICE}(t) + P_{Bat}(t) + P_{SC}(t) \quad (1)$$

Regarding a maximum global efficiency, ICE operations at better efficiency points are demanded and that occur at constant torque overall the speed range. Meanwhile, the SC responds to the power variations, storing the energy produced by the generator at standby phases and providing the excess for maneuvering operations. Battery is only used for zero-emission operation phases. The average power value and the extreme conditions to sizing the SC storage system are obtained by the analysis of the mission power diagram presented in Fig. 2. A charge sustaining method is also employed to guaranty that:

$$\frac{1}{T} \int_0^T P_{Bat}(t) dt = \frac{1}{T} \int_0^T P_{SC}(t) dt = 0 \quad (2)$$

The estimated SC power  $P_{SC}(t)$  over the mission period  $T$  is computed from the difference of power demand profile  $P_{dem}(t)$ , presented in Fig. 2, and its average  $P_{dem}$ , assigned to the diesel-generator  $P_{ICE}(t)$ , as depicted in (1). As an assumption, the power delivered by the supercapacitors will be then the same, with or without the battery operations, as proposed by:

$$P_{SC}(t) = P_{dem}(t) - P_{dem} \quad (3)$$

as

$$P_{dem} = \frac{1}{T} \int_0^T P_{dem}(t) dt = P_{ICE}(t) + P_{Bat}(t) \quad (4)$$

then

$$P_{dem} = \frac{1}{T} \int_0^T (P_{ICE}(t) + P_{Bat}(t)) dt \quad (5)$$

which, from (2), can be written as

$$P_{ICE} = \frac{1}{T} \int_0^T P_{ICE}(t) dt = P_{dem} \quad (6)$$

By (6), a constant diesel-generator power of 40.8kW can be set, and the power supported by the SC over the mission becomes the presented in Fig. 5. The maximum power requested to the SC is 67.2kW and during the storage operation the maximum power is - 40.8kW. The variation of energy stored and provided, in the SC system is 539.5Wh. Regarding voltage, current and energy constraints, the design of a suitable SC storage system for the ship mission can be based on several modules of 130F, 54V (M2-54V130F from BATSCAP). That results in the parallel of 2 branches of 7 modules in series.

#### 3.2. Sizing of the battery system for zero-emission operations

The battery system will be operated as a green energy boost system to avoid any emission during the casting-off and the docking operations of the excursion ship. Fig. 6a represents the increase of average power in the ICE with the quantity of energy embarked in the battery, computed using (7)–(9) where  $t_C$  is the time after the casting off maneuver and  $t_D$  is the time before the docking maneuver.  $P_{ICE-ref}$  corresponds to the constant power generated by the diesel-generator unit to obtain the average power demand for the on-time  $\Delta t_{ON}$  of the ICE. Fig. 6b defines the stop-time of the ICE regarding the energy stored in the battery system.

As proposed by Lhomme and Trovão in [15], for a hybrid system with just SCs system, the ICE output average power was set for 40.8kW, to maximize the usability of the SCs system, that it could be obtained in Fig. 6 for 0kWh of battery. In this paper, the design of the battery has been done to stop the ICE for

$\Delta t_{OFF} = 3$  min, that means 90s at the beginning of the power profile (casting-off) and 90s before the end of the trip (docking), as presented in Fig. 7.

Finally, considering voltage, current and energy constraints, a design of a suitable  $\Delta W_{bat} = 2$  kWh battery storage system for the proposed ship mission can be defined by:

$$P_{dem} = P_{ICE} = \frac{1}{T} \int_0^T P_{ICE}(t) dt = \frac{1}{T} \int_{t_C}^{t_D} P_{ICE-ref} dt \quad (7)$$

$$\begin{aligned} P_{ICE-ref} &= P_{dem} \frac{T}{\Delta t_{ON}} \text{ with } \Delta t_{ON} \\ &= T - \Delta t_{OFF} \\ &= t_D - t_C \end{aligned} \quad (8)$$

$$\Delta W_{bat} = P_{dem} \Delta t_{OFF} \quad (9)$$

The considered battery storage system for the green energy boost operations is based on 10 modules in series of 14.5Ah, 36V.

#### 4. Modeling and control of the excursion ship

Coupled to a diesel-electric topology an active association battery/SC is under study, as presented in Fig. 4. The overall description corresponds to a propulsion subsystem and a generation subsystem with a diesel-electric generator 90 hp (proposed by Lhomme and Trovão in [15] as an enhanced version of the original ship with 200 hp) plugged to a common DC bus, and in parallel with and active configuration of Battery/SC, as proposed in Fig. 4. Each ESS is connected to the DC bus by its own bidirectional DC-DC converter. Based on this specific configuration a simulation model is developed using EMR formalism for evaluation purpose of the sizing methodology and, finally, validate the zero-emission concept.

##### 4.1. Modeling and EMR of the excursion ship

EMR organizes the global system using four basic elements: energy sources (green ovals), energy accumulations (orange crossed rectangles), mono-physical (orange squares) and multi-physical conversions (orange circles) and energy distributions (double orange squares), as presented in Appendix. The basic elements are connected using the action-and-reaction principle. The product of the action-and-reaction variables provides the instantaneous power exchanged between the elements. All subsystems are modelled respecting the integral causality. The EMR is depicted in Fig. 8. The EMR of the Propulsion Subsystem (Ship M1 and Ship M2 in Fig. 4) is directly represented by an equivalent current source based on the power demand diagram presented in Fig. 2. The current  $i_{DC}$  is given by:

$$i_{DC}(t) = \frac{P_{dem}(t)}{v_{DC}(t)} \quad (10)$$

where  $v_{DC}$  is the voltage at the common DC bus. The DC bus capacitor is represented by an accumulation element. The common voltage  $v_{DC}$  is the state variable given by:

$$C_{DC} \frac{dv_{DC}(t)}{dt} = i_t(t) - i_{DC}(t) \quad (11)$$

where  $C_{DC}$  is the DC bus capacitor.

The ICE-generator, propulsion and ESS are coupled in parallel on the same common DC bus. The EMR representation is made by a coupling element to represent the parallel connection. The DC bus current ( $i_t$ ) is given by the sum of the currents  $i_{ch\_Bat}$ ,  $i_{ch\_SC}$  and the synchronous machine generator ( $i_{SM}$ ), keeping the same voltage  $v_{DC}$ :

$$\begin{cases} common v_{DC}(t) \\ i_t(t) = i_{SM}(t) + i_{ch\_SC}(t) + i_{ch\_Bat}(t) \end{cases} \quad (12)$$

The EMR of the ICE-generator subsystem is based on an ICE, a Synchronous Machine (SM) and a rectifier. The ICE transforms fuel into mechanical energy, represented as a controllable torque source and modelled by a quasi-static model. In this kind of model an equivalent dynamic model of the system, here a first-order system, is added into the steady-state model. A static map is then used to determine instantaneously the Brake Specific Fuel Consumption (BSFC) and emissions.

The ICE shaft is connected to the SM and it is represented by an accumulation element, which determines the speed  $\Omega_{SM}$  based on the ICE and SM torques, as presented in:

$$J_s \frac{d\Omega_{SM}(t)}{dt} + f_s \Omega_{SM}(t) = T_{ICE}(t) - T_{SM}(t) \quad (13)$$

where  $J_s$  and  $f_s$  is the inertia and the coefficient of friction, respectively, of the mechanical shaft.

The current  $i_{SM}$  is deduced from the supplied voltage  $v_{DC}$ , SM speed  $\Omega_{SM}$  and torque  $T_{SM}$ , using a static model of the electric drive, i.e. SM plus its rectifier and control, for efficiency computation ( $\eta_{SM}$ ), given by:

$$\begin{aligned} i_{SM}(t) &= \frac{T_{SM}(t)\Omega_{SM}(t)}{v_{DC}(t)\eta_{SM}^\beta(t)} \text{ with } \beta \\ &= \begin{cases} -1 & \text{for } T_{SM}(t)\Omega_{SM}(t) < 0 \\ 1 & \text{for } T_{SM}(t)\Omega_{SM}(t) \geq 0 \end{cases} \end{aligned} \quad (14)$$

A look-up table is used to define the efficiency  $\eta_{SM}$  from the torque  $T_{SM}$  and the rotation speed  $\Omega_{SM}$ . Regarding the ESS ( $j \in \{Bat, SC\}$ ), they are represented by a voltage source, which imposes the voltage of the ESS, as proposed by:

$$v_j(t) = v_j^{OCV}(t) - \frac{1}{C_j} \int i_j(t) dt - r_j i_j(t) \quad (15)$$

where  $v_j^{OCV}$  is the ESS initial open voltage.

The inductor of the DC/DC converter is represented by an accumulation element and modelled by:

$$v_j(t) = L_j \frac{di_j(t)}{dt} + r_{L_j} i_j(t) + v_{ch\_j}(t) \quad (16)$$

For the DC/DC converter the average model is used:

$$\begin{cases} v_{ch\_j}(t) = m_j(t)v_j(t) \\ i_{ch\_j}(t) = m_j(t)i_j(t)\eta_{ch_j}^\beta \end{cases} \text{ with } \beta \quad (17)$$

$$= \begin{cases} 1 & v_{DC}(t)i_{ch\_j}(t) \geq 0 \\ -1 & v_{DC}(t)i_{ch\_j}(t) < 0 \end{cases}$$

where  $m_j$  is the duty cycle of the pulse-width modulation and  $\eta_{ch_j}^\beta$  is the efficiency of each DC/DC converter.

##### 4.2. Control of the excursion ship

An inversion-based control is obtained directly by EMR (see light-blue pictograms of Fig. 8. The tuning path of the generation subsystem is defined and link the tuning variable ( $T_{SM\_ref}$ ) to the control objective variable ( $v_{DC}$ ). The DC bus model (11) is inverted using the DC bus controller  $C_v(t)$  to provide the reference current of the electric drive:

$$i_{t\_ref}(t) = i_{DC\_meas}(t) + C_v(t)(v_{DC\_ref}(t) - v_{DC\_meas}(t)) \quad (18)$$

The inversion of the SM drive is achieved by:

$$T_{SM\_ref}(t) = \frac{v_{DC\_meas}(t)i_{SM\_ref}(t)}{\Omega_{SM\_meas}(t)\eta_{SM}^\beta(t)} \quad (19)$$

Next, the shaft model (13) inversion requires the speed controller  $C_s(t)$  to provide a suitable ICE torque reference:

$$\begin{aligned} T_{ICE\_ref}(t) &= T_{SM\_meas}(t) \\ &\quad - C_s(t)(\Omega_{SM\_ref}(t) - \Omega_{SM\_meas}(t)) \end{aligned} \quad (20)$$

SM optimal speed reference is computed at an upper level, using the maximum efficiency for the power reference points and implemented in the block designed by "Strategy".

For the ESS control current, the  $i_{ch\_j\_ref}$  are given by:

$$i_{ch\_SC\_ref}(t) = i_{t\_ref}(t) - (i_{SM\_ref}(t) + i_{ch\_Bat\_ref}(t)) \quad (21)$$

To obtain the ESS current references an inversion of the conversion element (17) is used:

$$i_{j\_ref}(t) = \frac{i_{ch\_j\_ref}(t)}{m_j} \quad (22)$$



To compute  $v_{ch\_j\_ref}$  a current controller is required to invert (16):

$$v_{ch\_j\_ref}(t) = v_j(t) - C_{i\_j}(t) (i_{j\_ref}(t) - i_j(t)) \quad (23)$$

Finally,  $m_j$  is obtained using the inversion of (17), given by:

$$m_j(t) = \frac{v_{ch\_j}(t)}{v_{DC\_meas}(t)} \quad (24)$$

## 5. Simulation results and discussion

All the results have been obtained by MATLAB/Simulink™ simulation using EMR library. The simulation is carried out using the power demand evolution presented in Fig. 2 as DC bus dynamic load profile. For this study, a 90 hp diesel-engine efficiency map is used to compute the torque output as a function of shaft the rotational speed, as proposed by Lhomme and Trovão in [15]. The main parameters of the ESS are given in Table 1.

Two main results, without (see Fig. 9) and with battery (see Fig. 10), are presented. In this paper, only the results with battery can achieve zero-emission maneuvers. For both results the initial SC SoC is set to 86%. Due to the design of the SC, the same curves of SC voltage (Figs. 9d and 10d) and current are obtained (Figs. 9e and 10e). During the casting-off maneuver operation, the SC help the battery to supply the power demands to the casting-off maneuver. Naturally, its voltage decreases. During the cruising speed of the ship the SC only contribute during little fluctuation on the DC bus due to the quasi-constant power demanded by the propulsion (Figs. 9c and 10c). Near to the end of the mission, during the docking maneuver, the SC contribute again to the global power transition, charging and discharging several times.

Fig. 10 shows the results when the battery is used to avoid any emission during the docking and the casting-off maneuvers. At the beginning, during the casting-off maneuvers, only the battery (Fig. 10b) and SCs (Fig. 10e) propels the ship. The ICE is then turned on at 90 s with a constant power of 51 kW (Fig. 10a). At 810 s, just before the docking maneuver, the ICE is stopped. According to the power profile the SC will be charged or discharged by the battery. It might be noted that, without the battery ( $P_{bat} = 0$  in Fig. 9b), the ICE is always turned on and operates at its best operating point to deliver a power of 40.8 kW (Fig. 10a).

Fig. 11 shows the operating points of the ICE with (green star) and without (red star) battery. When the battery is not used the ICE works at its best consumption (210 g/kWh) for the operating point of 175 Nm, 2650 rpm. With the battery, the increase of the ICE power leads to a lower efficiency and a bit higher consumption (225 g/kWh) operation point. The fuel consumption is then higher when the battery is used: 2.85 l (+8%) with battery versus 2.64 l without battery. Nevertheless, even if the consumption increases a little, the use of the battery can avoid an emission of 1.39 kg of CO<sub>2</sub> during the casting-off and docking maneuvers.

The fuel consumption for different case studies are presented in Fig. 12. Globally, no reduction of the fuel consumption and emission are obtained keeping the ICE of 200 hp in a series hybrid configuration. Otherwise, when a decrease in power of the ICE is performed, for instance

using a 90 hp, an important reduction of 9.6% and 9.5% was computed, for fuel consumption and CO<sub>2</sub>, respectively. However, the zero-emission operations at casting-off and docking introduce a new energetic scenario and despite no emission are emitted during the maneuvers, the fuel consumption only decrease 2.4% in comparison to the original case. Another scenario could be the recharge of the battery at the dock during the entrance and the exit of the passengers. In this case the ICE will work at its best operating point (210 g/kWh) due to no recharges come from the ICE during the cruising of the ship. The battery will be used to propel the propulsion system during the casting-off and the docking phases with the energy stored when the ship was docked. The introduction of the plug-in option reduces the fuel consumption to a minimum of 2.33 l, and then the plug-in ship would allow a maximum reduction of 20.1% in fuel consumption, that implies a reduction of 20% in CO<sub>2</sub> emissions.

## 6. Conclusion

In this paper, a study on a possible enhancement of a diesel-electric excursion ship using EMR approach, devoted especially to ecological areas has been presented. A series hybrid configuration has been proposed using a hybrid ESS, with battery and supercapacitors, coupled to DC bus by an active topology. The use of the hybrid ESS allows zero-emission capabilities during the casting-off and the docking maneuvers, even without the clear advantage of regenerative braking energy. As demonstrated, EMR was central in the definition of the global control strategy to maximize the utility of the ESS and to set the best operation point of the ICE over the mission profile under the restriction of zero-emission. The main result was the reduction of the local CO<sub>2</sub> emission by 1.39 kg in the casting-off and docking maneuvers. However, the consumption of the ICE (and its emissions) increases (+8%) during the cruising speed phase. Although, the use of hybrid ESS and ICE operations at optimal points could be restored by the addition of plug-in capability to the ship. A reduction around 20% in consumption and emissions are observed. Local environmental benefits can be anticipated by these results for electric propulsion excursion ships with repetitive missions in sensitive areas. Future work will focus on more improved energy management strategies and multi-objective design of hybrid ESS to continuously expand the performance of the electric propulsion ships for sensitive areas.

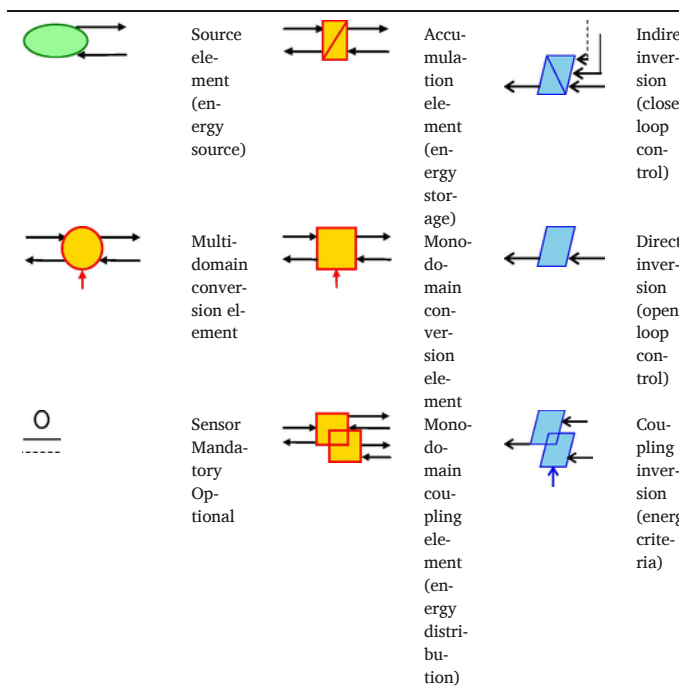
## Conflict of interest

None.

## Acknowledgments

This work was supported in part by the Natural Sciences and Engineering Research Council of Canada and was also partially supported by projects UID/MULTI/00308/2013 and by the European Regional Development Fund through the COMPETE 2020 Programme and FCT – Portuguese Foundation for Science and Technology within projects ESGRIDS (POCI-01-0145-FEDER-016434) and MAnAGER (POCI-01-0145-FEDER-028040).

Appendix: Summary of EMR pictograms



References

[1] E.S. Vagshlid, Adoption of mandatory energy efficiency measures for ships, Visit to IMO by Norwegian Shipping Forum, London, October 2012.

[2] G.A. Livanos, G. Theotokatos, D.N. Pagonis, Techno-economic investigation of alternative propulsion plants for Ferries and RoRo ships, *Energy Convers Manage* 79 (2014) 640–651.

[3] I. Shancita, H.H. Masjuki, M.A. Kalam, I.M. Rizwanul Fattah, M.M. Rashed, H.K. Rashedul, A review on idling reduction strategies to improve fuel economy and reduce exhaust emissions of transport vehicles, *Energy Convers Manage* 88 (2014) 794–807.

[4] G.G. Dimopoulos, C.A. Georgopoulou, I.C. Stefanatos, A.S. Zymaris, N.M.P. Kakalis, A general-purpose process modelling framework for marine energy systems, *Energy Convers Manage* 86 (2014) 325–339.

[5] J.F. Hansen, F. Wendt, History and state of the art in commercial electric ship propulsion, integrated power systems, and future trends, *Proc IEEE* 103 (12) (2015) 2229–2242.

[6] A. García-Olivares, J. Solé, O. Osychenko, “Transportation in a 100% renewable energy system”, *Energy Convers Manage* 158 (2018) 266–285.

[7] M. Cupelli, F. Ponci, G. Sulligoi, A. Vicenzutti, C.S. Edrington, T. El-Mezayani, et al., Power flow control and network stability in an all-electric ship, *Proc. IEEE* 103 (12) (2015) 2355–2380.

[8] G. Sulligoi, A. Vicenzutti, R. Menis, All electric ship design: from electrical propulsion to integrated electrical and electronic power systems, *IEEE Trans Transp Electr* 2 (4) (2016) 507–521.

[9] B. Guellard, X. De Montgros, P.P. De La Barriere, G. Wolfensberger, P. D’oliveira, “An overview of electric and solar boats market in France”, *World Electric Vehicle Symposium and Exhibition (EVS27)*, Barcelona (Spain), 20131–13.

[10] J.P. Trovão, F. Machado, P.G. Pereirinha, Hybrid electric excursion ships power supply system based on a multiple energy storage system, *IET Electr Syst Transp* 6 (3) (2016) 190–201.

[11] K. Bellache, M.B. Camara, Z. Zhou, B. Dakyo, “Energy management in hybrid electric boat based on frequency distribution approach – using diesel, lithium-battery and supercapacitors”, *2015 IEEE Vehicle Power and Propulsion Conference (VPPC)*, Montreal (Canada), 20151–6.

[12] J. Hou, J. Sun, H. Hofmann, “Interaction analysis and integrated control of hybrid energy storage and generator control system for electric ship propulsion”, *2015 American Control Conference (ACC)*, Chicago (USA), 20154988–4993.

[13] Z. Zhou, M.B. Camara, B. Dakyo, Coordinated power control of variable-speed diesel generators and lithium-battery on a hybrid electric boat, *IEEE Trans Vehicular Technol* 66 (7) (2017) 5775–5784.

[14] M.D.A. Al-Falahi, K.S. Nimma, S.D.G. Jayasinghe, H. Enshaei, J.M. Guerrero, Power management optimization of hybrid power systems in electric ferries, *Energy Convers Manage* 172 (2018) 50–66.

[15] W. Lhomme, J.P. Trovão, “Diesel-Electric Excursion Ships Enhancement using Energetic Macroscopic Representation”, *12th International Conference on Modeling and Simulation of Electric Machines, Converters and Systems, ELECTRIMACS 2017*, Toulouse, (France), 2017.

[16] Nguyen BH, German R, Trovão JPF, Bouscayrol A, “Real-time energy management of battery/supercapacitor electric vehicles based on an adaptation of pontryagin’s minimum principle”, *IEEE Trans. on Vehicular Technology*, early access.

[17] J. Shen, S. Dusmez, A. Khaligh, Optimization of sizing and battery cycle life in battery/UC hybrid energy storage system for electric vehicle applications, *IEEE Trans Ind Informat* 10 (4) (2014) 2112–2121.

[18] A. Ostadi, M. Kazerani, A comparative analysis of optimal sizing of battery-only, ultracapacitor-only, and battery-ultracapacitor hybrid energy storage systems for a city bus, *IEEE Trans Veh Technol* 64 (10) (2015) 4449–4460.

[19] R.E. Araújo, R. De Castro, C. Pinto, P. Melo, D. Freitas, Combined sizing and energy management in EVs with batteries and supercapacitors, *IEEE Trans Vehicular Technol* 63 (7) (2014) 3062–3076.

[20] L. Zhang, X. Hu, Z. Wang, F. Sun, J. Deng, D.G. Dorrell, Multiobjective optimal sizing of hybrid energy storage system for electric vehicles, *IEEE Trans Vehicular Technol* 67 (2) (2018) 1027–1035.

[21] X. Wu, X. Hu, Y. Teng, S. Qian, R. Cheng, Optimal integration of a hybrid solar-battery power source into smart home nanogrid with plug-in electric vehicle, *J Power Sources* 363 (2017) 277–283.

[22] C.M. Martinez, X. Hu, D. Cao, E. Velenis, B. Gao, M. Wellers, Energy management in plug-in hybrid electric vehicles: recent progress and a connected vehicles perspective, *IEEE Trans Vehicular Technol* 66 (6) (2017) 4534–4549.

[23] A. Bouscayrol, J.P. Hautier, B. Lemaire-Semail, “Graphic formalisms for the control of multi-physical energetic systems: COG and EMR”, *Systemic Design Methodologies for Electrical Energy Systems: Analysis, Synthesis and Management*, John Wiley & Sons Inc, Hoboken, NJ, USA, 2012.

[24] A.L. Allègre, P. Delarue, P. Barrade, A. Bouscayrol, E. Chattot, S. El-Fassi, Influence of the mechanical limitations of a traction system on energy storage design, *Math Comput Simul* 81 (2) (2010) 302–314.

[25] C. Mayet, J. Pouget, A. Bouscayrol, W. Lhomme, Influence of an energy storage system on the energy consumption of a diesel-electric locomotive, *IEEE Trans Vehicular Technol* 63 (3) (2014) 1032–1040.

[26] W. Borutzky, G. Dauphin-Tanguy, J.U. Thoma, Advances in bond graph modelling: theory, software, applications, *Math Comput Simul* 39 (5–6) (1995) 465–475.